

Efficient finite element model for dynamic analysis of laminated composite beam

M. Naushad Alam*, Nirbhay Kr. Upadhyay and Mohd. Anas

Department of Mechanical Engineering, Aligarh Muslim University, Aligarh-202002, India

(Received February 21, 2011, Revised March 27, 2012, Accepted April 11, 2012)

Abstract. An efficient one dimensional finite element model has been presented for the dynamic analysis of composite laminated beams, using the efficient layerwise zigzag theory. To meet the convergence requirements for the weak integral formulation, cubic Hermite interpolation is used for the transverse displacement (w_0), and linear interpolation is used for the axial displacement (u_0) and shear rotation (ψ_0). Each node of an element has four degrees of freedom. The expressions of variationally consistent inertia, stiffness matrices and the load vector are derived in closed form using exact integration. The formulation is validated by comparing the results with the 2D-FE results for composite symmetric and sandwich beams with various end conditions. The employed finite element model is free of shear locking. The present zigzag finite element results for natural frequencies, mode shapes of cantilever and clamped-clamped beams are obtained with a one-dimensional finite element codes developed in MATLAB. These 1D-FE results for cantilever and clamped beams are compared with the 2D-FE results obtained using ABAQUS to show the accuracy of the developed MATLAB code, for zigzag theory for these boundary conditions. This comparison establishes the accuracy of zigzag finite element analysis for dynamic response under given boundary conditions.

Keywords: composite laminates; FEM, MATLAB; dynamic analysis; ABAQUS

1. Introduction

Increasing demand for the development of light weight and reliable structure particularly in space technology, automobile, turbo machinery and marine structures are some of the examples where composites can be often used. Analysis and design of such laminated structures requires an accurate and efficient model. The finite element (FE) method provides a powerful tool for the numerical analysis of composite structures. Aircraft wings, turbo machinery blades, space and marine structures can be modeled as composite or sandwich beams. Substantial literatures are available in this area. Benjeddou (2000) reviewed finite element modeling of laminated elastic substrate with piezoelectric layers. He concluded that the analysis of these laminate requires efficient and accurate approximation of the displacement across the thickness. Robbins and Reddy (1991) presented dynamic and static finite element analysis of hybrid beams using discrete layerwise theory with piecewise linear approximation of displacement across the thickness. Averill and Yip (1996) presented thick beam theory and finite element model with zigzag theory. Mackerle (2003)

*Corresponding author, Associate Professor, E-mail: naushad7863@rediffmail.com

presented a finite element approach for smart materials and structures. Chopra (2002) presented state of the art review on smart structures and integrated systems. Averill (1994) presented a static and dynamic response of moderately thick laminated beams with damage. Cho and Parmerter (1992) presented efficient higher order plate theory for general lamination configuration. Navier type solutions for simply supported beams are presented by Kapuria *et al.* (2004, 2005) which do not provide finite element formulation of zigzag theory. Kapuria and Alam (2006) presented efficient layerwise finite element model for dynamic analysis of laminated piezoelectric beams.

Arya *et al.* (2002) presented a model that uses a sine term to represent the nonlinear displacement field across the thickness as compared to a third order polynomial term in conventional theories. Transverse shear stress and strain are represented by a cosine term as compared to parabolic term. They given analytical results for cross ply laminate. Akhras and Li (2007) presented spline finite strip method for static analysis of composite plates using the higher-order zigzag theory for composite plate. Fares and Elmarghany (2008) presented refined nonlinear zigzag shear deformation theory of composite laminated plates using a modified mixed variational formulation. Their theory accounts for continuous piecewise layer-by-layer linear variation approximation in the thickness direction for the displacements. Kumari *et al.* (2008) presented a new improved third order theory (ITOT) for hybrid piezoelectric angle-ply flat panels under thermal loading. The ITOT and the existing efficient zigzag theory are assessed for simply-supported angle-ply flat hybrid panels for static loads and for natural frequencies by comparison with 2D solutions. Kapuria and Achary (2008) have developed a benchmark 3D solution and assessment of a zigzag theory for free vibration of hybrid plates under initial electro-thermo-mechanical stresses. Kapuria *et al.* (2008) has given a third order zigzag theory based model for layered functionally graded beams in conjunction with the modified rule of mixtures (MROM) for effective modulus of elasticity is validated through experiments for static and free vibration response.

This work presents finite element model based on zigzag theory, for the analysis of composite beams, by extending the work of Kapuria *et al.* (2004) for various boundary conditions. The weak form of integration consistent with element mass matrix and stiffness matrices is derived for this purpose. The present 1D- Finite Element model is validated by comparing the dynamic response with 2D-Finite Element model using ABAQUS software. Cubic Hermite interpolation is used for deflection, and linear interpolation is used for axial displacement and shear rotation. Natural frequencies and mode shapes for composite and sandwich beams are presented. The present results for cantilever and clamped beams are compared with the 2D-FE results obtained using ABAQUS. This shows the accuracy of the developed MATLAB code for zigzag theory, for these boundary conditions.

2. The displacement field and variational equation

A laminated composite beam (Fig. 1) of width b , thickness h and length l , made of L perfectly bonded orthotropic layers with longitudinal axis x , is considered. For a beam of uniform cross-section, the mid-plane of the beam is chosen as the xy -plane.

Let the planes $z = z_0$ and $z = z_L$ be the bottom and top surfaces of the beam. For a uniform beam, $z_0 = -h/2$ and $z_L = h/2$. The z -coordinate of the bottom surface of the k th layer from the bottom is denoted as z_{k-1} and its material symmetry direction 1 is at an angle θ_k to the x -axis. The reference plane $z = 0$ either passes through or is the bottom surface of the k_0^{th} layer.

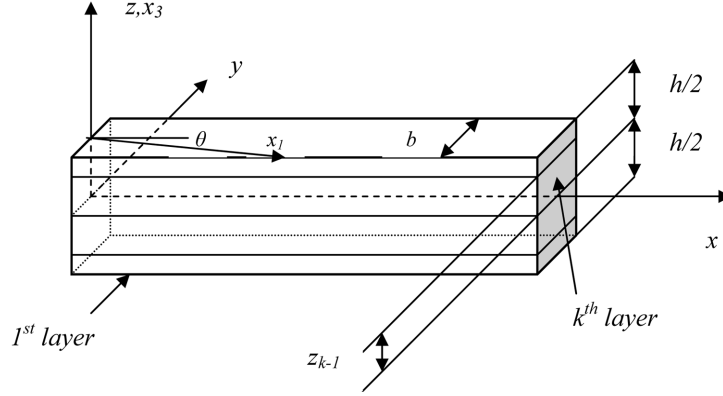


Fig. 1 Geometry of a laminated composite beam

The strain displacement relations for directions x, z , including geometric non linearity due to w are

$$\varepsilon_x = u_{,x} + \frac{1}{2}w_{0,x}^2, \quad \varepsilon_z = w_{,z}, \quad \gamma_{zx} = u_{,z} + w_{,x} \quad (1)$$

The constitutive equations for the stresses are

$$\sigma_x = \hat{Q}_{11} \cdot \varepsilon_x, \quad \tau_{zx} = \hat{Q}_{55} \cdot \gamma_{zx} \quad (2)$$

where, $\hat{Q}_{11}, \hat{Q}_{55}$ are the stiffnesses which are given in terms of material properties and orientation of material property axis 1 with respect to beam axis x .

The transverse deflection is approximated to be independent of z , i.e.,

$$w(x, z, t) = w_0(x, t) \quad (3)$$

For the k 'th layer, longitudinal displacement u is approximated Kapuria *et al.* (2004) as

$$u(x, z, t) = u_k(x, t) - z \cdot w_{0,x}(x, t) + z \cdot \psi_k(x, t) + z^2 \cdot \xi(x, t) + z^3 \cdot \eta(x, t) \quad (4)$$

The functions u_k, ψ_k, ξ, η are expressed in terms of primary variables $u_0(x, t) = u_{k_0}(x, t) = u(x, 0, t)$ and $\psi_0(x, t) = \psi_{k_0}(x, t)$ using $(L-1)$ conditions each for the continuity of τ_{zx} and u at the layer interfaces and the two shear traction free conditions $\tau_{zx} = 0$ at the top and bottom surfaces at $z = z_0, z_L$. Using these, the expression of u takes the form as

$$u(x, z, t) = u_0(x, t) - z \cdot w_{0,x}(x, t) + R^k(z) \cdot \psi_0(x, t) \quad (5)$$

Where,

$$\begin{aligned} R^k(z) &= R_k(z)/R_2^{k_0} = \hat{R}_1^k + z \cdot \hat{R}_2^k + z^2 \cdot \hat{R}_3^k + z^3 \cdot \hat{R}_4^k \\ (\hat{R}_1^k, \hat{R}_2^k, \hat{R}_3^k, \hat{R}_4^k) &= (R_1^k, R_2^k, R_3^k, R_4^k)/R_2^{k_0} \\ R_k(z) &= R_1^k + z \cdot R_2^k + z^2 \cdot R_3^k + z^3 \cdot R_4^k, \quad R_1^k = \bar{R}_2^k - \bar{R}_2^{k_0} \end{aligned}$$

$$\begin{aligned} \bar{R}_2^k &= \sum_{i=2}^k (R_2^{i-1} - R_2^i) \cdot z_{i-1}, \quad R_2^k = a_1^k \cdot R_3 + a_2^k \cdot R_4 \\ a_1^k &= 2(C_1^k / Q_{55}^k - z_k), \quad a_2^k = 3(2C_2^k / Q_{55}^k - z_k^2) \\ R_3 &= \frac{4C_2^L}{\Delta}, \quad R_4 = \frac{-4C_1^L}{3\Delta}, \quad \Delta = 4z_0^2 C_1^L - 8z_0 C_2^L \end{aligned}$$

The variational equation for developing element matrices of FE model is derived from the Hamilton's Principle

$$\int_{t_1}^{t_2} \left[\int_V (\rho \dot{u}_i \delta \dot{u}_i - \sigma_{ij} \delta \varepsilon_{ij}) dV + \int_{\Gamma} T_i^n \delta u_i d\Gamma \right] dt = 0 \tag{6}$$

Let p_z^1 and p_z^2 be the forces per unit area applied on the bottom and top surfaces of the beam in direction z . Using the following notation for integration along thickness

$$\langle \dots \rangle = \sum_{k=1}^L \int_{z_{k-1}}^{z_k} (\dots) b dz \tag{7}$$

and displacement field given by Eqs. (3) and (5) into the Eq.(6), reduces to the following variational form in terms of beam variables

$$\begin{aligned} &\int_0^l [\delta \bar{u}_1^T I \cdot \ddot{\bar{u}}_1^T + \delta w_0 \bar{I}_{22} \ddot{w}_0 + \delta u_{0,x} N_x - \delta w_{0,xx} M_x + \delta \psi_{0,x} P_x + \delta \psi_0 Q_x + \delta w_{0,x} N_x w_{0,x} - F_2 \delta w_0] dx \\ &- [N_x^* \delta u_0^* + V_x^* \delta w_0^* - M_x^* \delta w_{0,x}^* + P_x^* \delta \psi_0^*]_0^l = 0 \end{aligned} \tag{8}$$

where, the superscript * means the values at the ends.

The beam stress resultants F_1 of σ_x and Q_x, V_x of τ_{zx} are defined by

$$F_1 = \langle f_1^T(z) \cdot \sigma_x \rangle = \begin{bmatrix} N_x \\ M_x \\ P_x \end{bmatrix} = \begin{bmatrix} \langle \sigma_x \rangle \\ \langle z \cdot \sigma_x \rangle \\ \langle R^k(z) \cdot \sigma_x \rangle \end{bmatrix}, \quad \begin{aligned} V_x &= \langle \tau_{zx} \rangle \\ Q_x &= \langle R_{,z}^k(z) \cdot \tau_{zx} \rangle \end{aligned} \tag{9}$$

$$F_2 = b(p_z^1 + p_z^2)$$

3. Finite element model

Two noded elements have been used for the primary displacement variables. The primary variables u_0, w_0, ψ_0 within an element are expressed in terms of their nodal values using appropriate polynomial interpolation functions. The highest derivatives of u_0, w_0, ψ_0 appearing in the variational Eq. (8) are $u_{0,x}, w_{0,xx}, \psi_{0,x}$. To meet the convergence requirements of the finite element method u_0, ψ_0 is C^0 Continuous and w_0 satisfies C^1 Continuity at the element boundaries. Hence w_0 is expanded using cubic Hermite interpolation along x and linear Lagrange interpolation along x is used for u_0, ψ_0 . The shear strain in Eq. (1) is dependent only on ψ_0 so that the used interpolation scheme will not undergo any shear locking. Thus at element level, each node will have four degrees

of freedom $u_0, w_0, w_{0,x}, \psi_0$ for the displacement. The value of an entity (...) at the nodes 1 and 2 is denoted by $(\dots)_1$ and $(\dots)_2$ respectively.

The following interpolations of u_0, w_0, ψ_0 are used in terms of the nodal values and the shape function matrices N, \bar{N}

$$\begin{aligned} u_0 &= N.u_0^e \\ \psi_0 &= N.\psi_0^e \\ w_0 &= \bar{N}.w_0^e \end{aligned} \tag{10}$$

With

$$u_0^e = \begin{bmatrix} u_{0_1} \\ u_{0_2} \end{bmatrix}, \quad \psi_0^e = \begin{bmatrix} \psi_{0_1} \\ \psi_{0_2} \end{bmatrix}, \quad w_0^e = \begin{bmatrix} w_{0_1} \\ w_{0,x_1} \\ w_{0_2} \\ w_{0,x_2} \end{bmatrix} \tag{11}$$

$$N = [N_1 \ N_2], \quad \bar{N} = [\bar{N}_1 \ \bar{N}_2 \ \bar{N}_3 \ \bar{N}_4] \tag{12}$$

$$N_1 = 1 - \frac{x}{L_e}, \quad N_2 = \frac{x}{L_e}$$

$$\bar{N}_1 = 1 - \frac{3x^2}{L_e^2} + \frac{2x^3}{L_e^3}, \quad \bar{N}_2 = x - \frac{2x^2}{L_e} + \frac{x^3}{L_e^2}$$

$$\bar{N}_3 = \frac{3x^2}{L_e^2} - \frac{2x^3}{L_e^3}, \quad \bar{N}_4 = -\frac{x^2}{L_e} + \frac{x^3}{L_e^2} \tag{13}$$

The integrand in the variational Eq. (8), for the case of static mechanical load, can be expressed as

$$[\delta \bar{u}_1^T \ \delta \bar{u}_2^T] \cdot \begin{bmatrix} I & 0 \\ 0 & \bar{I}_{22} \end{bmatrix} \cdot \begin{bmatrix} \ddot{u}_1 \\ \ddot{u}_2 \end{bmatrix} + [\delta \bar{\varepsilon}_1^T \ \delta \bar{\varepsilon}_5^T] \cdot \begin{bmatrix} A & 0 \\ 0 & A \end{bmatrix} \cdot \begin{bmatrix} \bar{\varepsilon}_1 \\ \bar{\varepsilon}_5 \end{bmatrix} - \delta w_0 \cdot F_2 \tag{14}$$

Hence, the contribution T_L^e of one element of length L_e to the integral in Eq.(8) is

$$T_L^e = \int_0^{L_e} [\delta \hat{u}^T \hat{I} \hat{\ddot{u}} + \delta \hat{\varepsilon}^T \hat{D} \hat{\varepsilon} - \delta \bar{u}_2 F_2] dx \tag{15}$$

where

$$\hat{u} = \begin{bmatrix} \bar{u}_1 \\ \bar{u}_2 \end{bmatrix} = [u_0 \ -w_{0,x} \ \psi_0 \ w_0]^T, \quad \bar{u}_2 = w_0$$

$$\hat{\varepsilon} = \begin{bmatrix} \bar{\varepsilon}_1 \\ \bar{\varepsilon}_5 \end{bmatrix} = [u_{0,x} \ -w_{0,xx} \ \psi_{0,x} \ \psi_0]^T \tag{16}$$

$$F_2 = b(p_z^1 + p_z^2)$$

$$\hat{I} = \begin{bmatrix} I & 0 \\ 0 & \bar{I}_{22} \end{bmatrix}, \quad \hat{D} = \begin{bmatrix} A & 0 \\ 0 & \bar{A} \end{bmatrix}, \quad \hat{F} = \begin{bmatrix} F_1 \\ F_5 \end{bmatrix} = \hat{D}\hat{\varepsilon} \quad (17)$$

$\hat{u}, \hat{\varepsilon}$ are the generalized displacement and generalized strains of the beam, \hat{I} is the beam inertia matrix and \hat{F} is the generalized stress vector of the beam. \hat{F} is related to $\hat{\varepsilon}$ by the generalized stiffness matrix \hat{D} of the beam. A, \bar{A} are defined in terms of material constants.

The element generalized displacement vector U^e is

$$U^e = [u_0^{eT} \quad w_0^{eT} \quad \psi_0^{eT}]^T \quad (18)$$

The beam generalized displacements $\bar{u}_1, \bar{u}_2, \hat{u}$ are related to U^e by B_{m_1}, B_{m_2}, B_m

$$\begin{aligned} \bar{u}_1 &= B_{m_1} \cdot U^e \\ \bar{u}_2 &= B_{m_2} \cdot U^e \\ \hat{u} &= B_m \cdot U^e \end{aligned} \quad (19)$$

$$B_{m_1} = \begin{bmatrix} N & 0 & 0 \\ 0 & -\bar{N}_{,x} & 0 \\ 0 & 0 & N \end{bmatrix}, \quad B_{m_2} = [0 \quad \bar{N} \quad 0]$$

$$B_m = \begin{bmatrix} B_{m_1} \\ B_{m_2} \end{bmatrix} = \begin{bmatrix} N & 0 & 0 \\ 0 & -\bar{N}_{,x} & 0 \\ 0 & 0 & N \\ 0 & \bar{N} & 0 \end{bmatrix} \quad (20)$$

$$\hat{\varepsilon} = \hat{B} \cdot U^e \quad (21)$$

where

$$\hat{B} = \begin{bmatrix} N_{,x} & 0 & 0 \\ 0 & -\bar{N}_{,xx} & 0 \\ 0 & 0 & N_{,x} \\ 0 & 0 & 0 \end{bmatrix} \quad (22)$$

Using Eq. (19) for \hat{u} and \bar{u}_2 and Eq. (21) for $\hat{\varepsilon}$ in Eq. (15), T_L^e can be expressed as

$$\begin{aligned} T_L^e &= \int_0^{L_c} \delta U^{eT} [B_m^T \cdot \hat{I} \cdot B_m \cdot \ddot{U}^e + \hat{B}^T \cdot \hat{D} \cdot \hat{B} \cdot U^e - B_{m_2}^T \cdot F_2] dx \\ &= \delta U^{eT} \cdot [M^e \cdot \ddot{U}^e + K^e \cdot U^e - P^e] \end{aligned} \quad (23)$$

with

$$M^e = \int_0^{L_e} B_m^T \hat{I} B_m dx \quad (24)$$

$$K^e = \int_0^{L_e} \hat{B}^T \hat{D} \hat{B} dx \quad (25)$$

$$P^e = \int_0^{L_e} B_{m_2}^T F_2 dx \quad (26)$$

The elements of element inertia matrix M^e , element stiffness matrix K^e and element load vector P^e are listed in the appendix.

Summing up contributions of all elements to the integral in Eq. (8), the system equation can be obtained as

$$M\ddot{U} + KU = P \quad (27)$$

in which M , K and P are assembled from the element matrices M^e , K^e and P^e .

The boundary conditions for a movable simply supported end, immovable simply supported (hinged) end, clamped end and free end are as follows:

Simply supported end

$$\begin{aligned} N_x = 0, (\text{movable}) & & u_0 = 0, (\text{immovable}) \\ w_0 = 0 & & M_x = 0 \\ P_x = 0 & & \end{aligned} \quad (28)$$

Clamped end

$$u_0 = w_0 = w_{0,x} = \psi_0 = 0 \quad (29)$$

Free end

$$\begin{aligned} N_x = N_x^*, \quad M_x = M_x^* \\ P_x = P_x^*, \quad V_x = V_x^* \end{aligned} \quad (30)$$

4. Results and discussion

Three laminated beams (a) and (b) and (c) are analyzed here. The stacking order is mentioned from the bottom. Beam (a) is a composite beam of material 1 Tang *et al.* (1996) consisting of four plies of equal thicknesses 0.25 h. Beam (a) has symmetric layup $[0^\circ/90^\circ/90^\circ/0^\circ]$. The three layer sandwich beam (b) has Graphite-epoxy faces and a soft core Noor and Burton (1994) with thicknesses 0.1 h/0.8 h/0.1 h. The orientation angle $\theta_k = 0^\circ$, for all the plies of beams (b). Beam (c) is an angle ply composite beam of material 1 consisting of four plies of equal thicknesses 0.25 h having symmetric lay ups $[0^\circ, 15^\circ, 30^\circ, 45^\circ, 60^\circ, 90^\circ]$.

Table 1 Material properties of the beams

Property	Units	Material (1)	Face	Core
Y_1	GPa	181.0	131.1	0.0002208
Y_2	GPa	10.3	6.9	0.0002001
Y_3	GPa	10.3	6.9	2.760
G_{12}	GPa	7.17	3.588	0.01656
G_{23}	GPa	2.87	2.3322	0.4554
G_{31}	GPa	7.17	3.588	0.5451
ν_{12}	-	0.28	0.32	0.99
ν_{13}	-	0.28	0.32	3×10^{-5}
ν_{23}	-	0.33	0.49	3×10^{-5}
ρ	kg/m ³	1578	1000	70

The material properties for the above mentioned beams are given in Table 1.

For a beam of span ' l ' and thickness ' h ', the thickness parameter $S = l/h$.

In this section, 2D-FE results are obtained for laminated composite beam (a) and (c) and sandwich beam (b) using the *ABAQUS* package (2007) for dynamic response. For the 2D-Finite element analysis using *ABAQUS 6.6*, composite beam (a) and (c) have been discretized into 2000 eight noded plane stress elements (CPS8R) for $S = 20, 50, 100, 200$. Same number of elements has been used for discretizing sandwich beam (b). The results obtained using twice the above numbers of elements are found to be indistinguishable from these results.

A 1D-FE MATLAB program have been developed for computing flexural natural frequencies of laminated composite beams which computes natural frequencies and mode shapes for various boundary conditions viz., cantilever and fixed. The natural frequency of n th longitudinal mode is non-dimensionalized as follows,

$$\bar{\omega}_n = \omega_n l s (\rho_0 / Y_0)^{1/2}$$

with $Y_0 = 10.3$ GPa for beam (a) and (c) and $Y_0 = 6.9$ GPa for beams (b), $\rho_0 = 1578$ kg/m³ for

Table 2 2D and 1D-FE results for flexural natural frequencies $\bar{\omega}_n$ of cantilever beams

S	Mode n	Composite beam (a)			Sandwich beam (b)		
		2D-FE	1D-FE	% error	2D-FE	1D-FE	% error
20	1	3.896	3.897	0.02	5.787	5.789	0.05
	2	21.490	21.545	0.25	28.664	28.750	0.29
	3	51.935	52.203	0.51	64.456	64.753	0.45
50	1	3.979	3.979	0.00	6.053	6.053	0.00
	2	24.345	24.350	0.02	36.050	36.070	0.05
	3	65.737	65.766	0.04	93.980	94.078	0.10
100	1	3.992	3.992	0.00	6.094	6.094	0.02
	2	24.860	24.863	0.01	37.685	37.689	0.01
	3	68.936	68.939	0.004	103.330	103.370	0.04
200	1	3.995	3.995	0.003	6.105	6.105	0.00
	2	24.998	24.998	0.00	38.128	38.130	0.005
	3	69.820	69.820	0.00	106.180	106.190	0.009

beam (a) and (c) and for beam (b) $\rho_0 = 1000 \text{ kg/m}^3$.

First three flexural natural frequencies have been computed using this program for composite beam (a), angle ply beam (c) and sandwich beam (b), for cantilever and fixed boundary conditions. For converged results beam (a) has been discretized into 150 elements while beam (b) into 140 elements. All results of $\bar{\omega}_n$ have been taken with 150 elements for beam (a) and 140 elements for beam (b). Convergence is faster for the earlier modes. The percentage error of these results from the 2D-FE results obtained by ABAQUS is listed along with 2D-FE results in Table 2 for cantilever beams and in Table 3 for fixed beams. In Table 4 results have been presented for angle ply beam (c) for flexural natural frequencies and their error for various thicknesses to span ratios. In Figs. 2-4, percentage error in flexural natural frequencies is plotted against thickness parameter for cantilever

Table 3 2D and 1D-FE results for flexural natural frequencies $\bar{\omega}_n$ of fixed beams

S	Mode n	Composite beam (a)			Sandwich beam (b)		
		2D-FE	1D-FE	% error	2D-FE	1D-FE	% error
20	1	20.505	20.590	0.41	26.270	26.380	0.41
	2	47.647	48.077	0.89	56.800	57.205	0.70
	3	80.327	81.368	1.27	92.196	92.976	0.83
50	1	24.385	24.393	0.03	35.606	35.633	0.07
	2	64.194	64.340	0.22	89.842	89.995	0.17
	3	119.230	119.440	0.17	160.255	160.680	0.26
100	1	25.153	25.155	0.007	37.970	37.976	0.01
	2	68.467	68.467	0.00	101.880	101.930	0.04
	3	132.030	132.080	0.037	193.391	193.390	0.0005
200	1	25.359	25.359	0.001	38.718	38.640	0.20
	2	69.675	69.675	0.00	105.752	105.760	0.007
	3	136.020	136.010	0.007	205.449	205.470	0.01

Table 4 2D and 1D-FE results for flexural natural frequencies $\bar{\omega}_n$ of angle ply symmetric cantilever beam (c)

S	Mode n	Composite beam (c) for 45°			Composite beam (c) for 60°		
		2D-FE	1D-FE	% error	2D-FE	1D-FE	% error
20	1	3.973	3.9307	-1.06	3.882	3.9121	.077
	2	23.745	22.310	-6.04	23.046	21.9088	-5.19
	3	62.188	56.290	-9.48	59.780	53.6531	-11.49
50	1	3.932	3.9937	-1.54	3.925	3.984	1.49
	2	24.500	24.577	-0.31	24.416	24.452	0.15
	3	67.300	66.932	-0.54	67.58	66.315	0.03
100	1	4.005	4.0031	-0.05	3.978	3.995	0.43
	2	25.048	24.970	-0.31	24.869	24.906	0.15
	3	69.906	69.402	-0.72	69.357	69.140	-.31
200	1	3.936	4.005	1.73	3.931	3.998	1.69
	2	24.650	25.072	1.68	24.62	25.024	1.61
	3	69.009	70.070	1.51	68.89	69.915	1.46

end conditions. In Figs. 5-7, percentage error in flexural natural frequencies is plotted against thickness parameter for fixed end conditions. Mode shapes for the first three flexural modes obtained by 1D-FE analysis, are also compared with the same obtained by 2D-FE for cantilever and fixed beams (a) and (b) with $S = 10$. These comparisons are shown in Figs. 8-11.

For cantilever beams, the maximum percentage errors in first, second and third natural frequency are .02%, 0.26%, 0.54% (all for $S = 20$, beam (a)). For fixed beams, the maximum percentage errors in first, second and third natural frequency are 0.41%, 0.92%, 1.33% (all for $S = 20$, beam (a)). With $S \geq 100$, for fixed beams, the maximum percentage errors in first, second and third natural

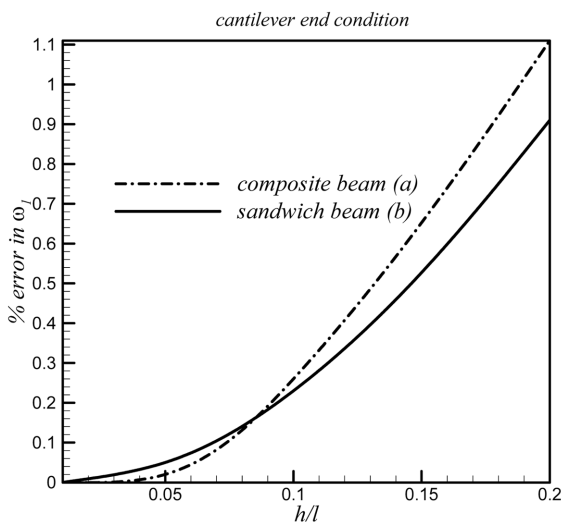


Fig. 2 % error in $\bar{\omega}_1$ for cantilever beam (a) and (b)

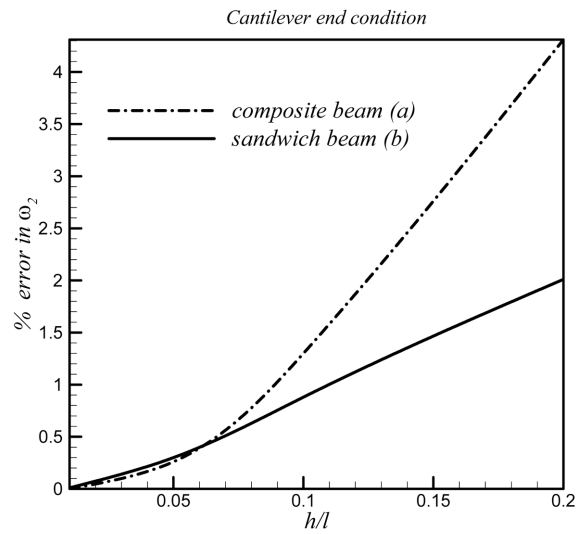


Fig. 3 % error in $\bar{\omega}_2$ for cantilever beam (a) and (b)

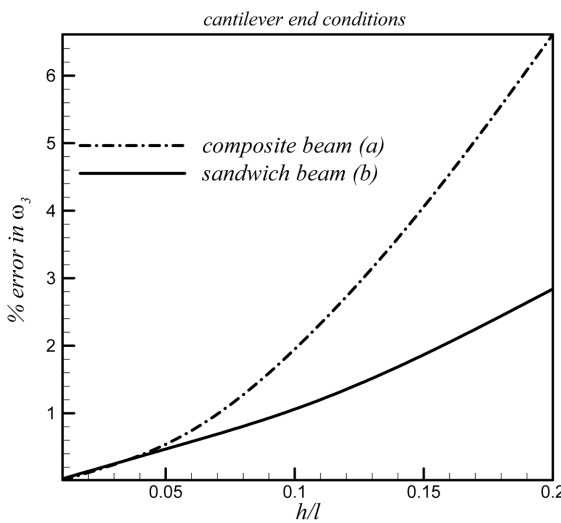


Fig. 4 % error in $\bar{\omega}_3$ for cantilever beam (a) and (b)

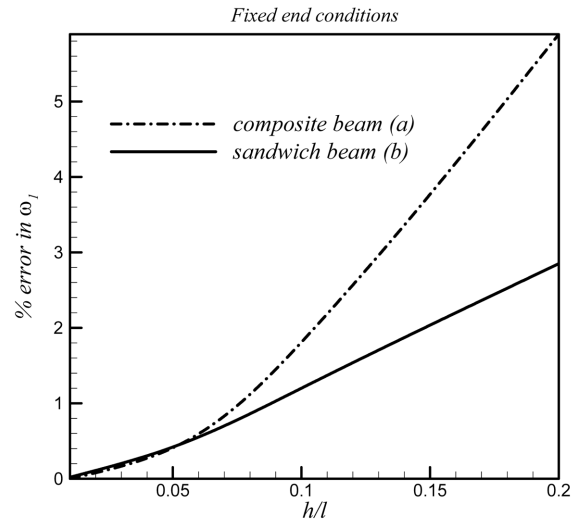


Fig. 5 % error in $\bar{\omega}_1$ for fixed beams (a) and (b)

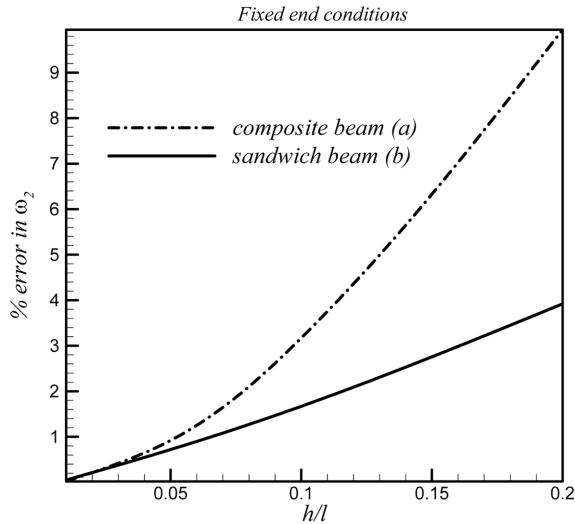


Fig. 6 % error in $\bar{\omega}_2$ for fixed beams (a) and (b)

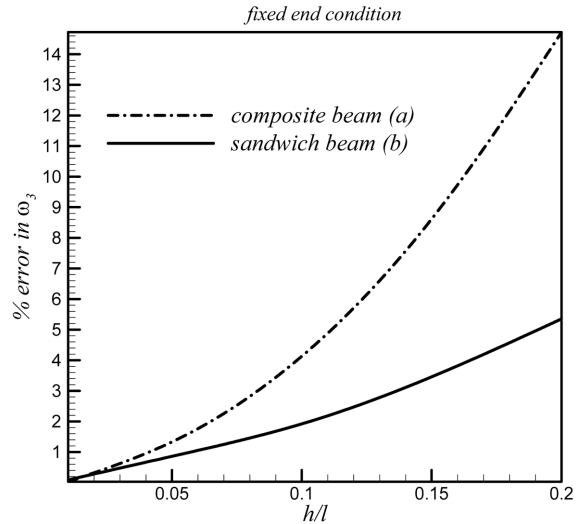


Fig. 7 % error in $\bar{\omega}_3$ for fixed beams (a) and (b)

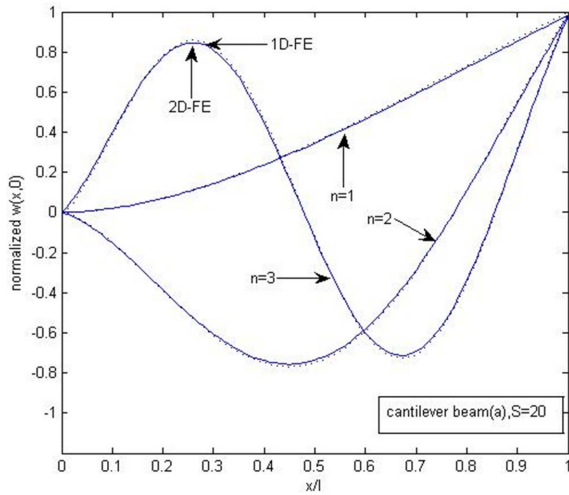


Fig. 8 Comparison of flexural mode shapes for cantilever composite beam (a)

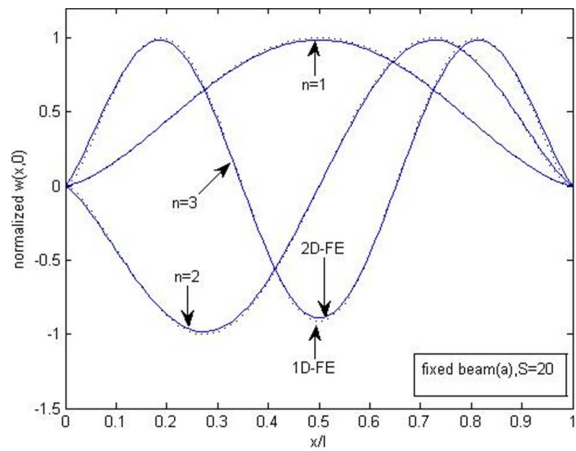


Fig. 9 Comparison of flexural mode shapes for fixed composite beam (a)

frequencies are 0%, .02%, .03%. The effect of ply angle on first frequency is shown in Fig. 12 and on second frequency is presented in Fig. 13. The plot shows that there is a marginal effect on angle up to 30. After 30 the frequency stabilizes. The mode shapes of 1D-FE as compared in Figs. 8-11 are also very close to the same of 2D-FE (ABAQUS). In Fig. 15, the first three flexural bending modes for fixed sandwich beam (b), with $S = 20$, are shown in *ABAQUS* environment as a screen shot. The screen shot is giving the similar trend for beam (b) as given by 1D-FE theory.

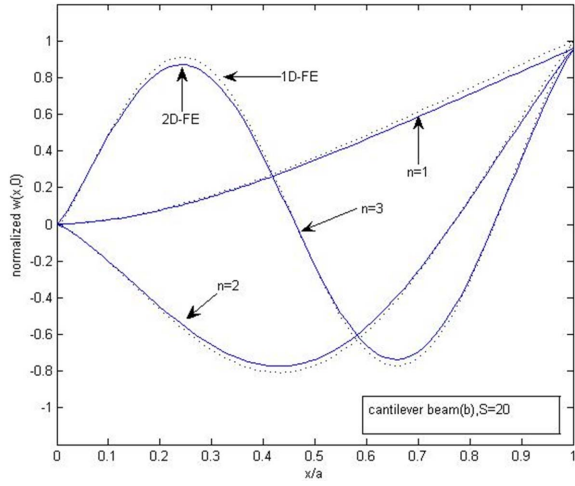


Fig. 10 Comparison of flexural mode shapes for cantilever sandwich beam (b)

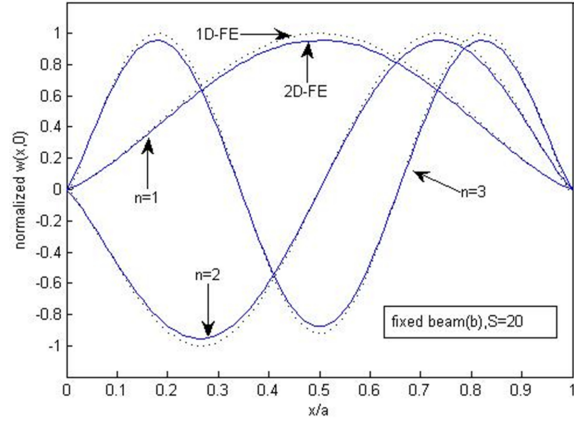


Fig. 11 Comparison of flexural mode shapes for fixed sandwich beam (b)

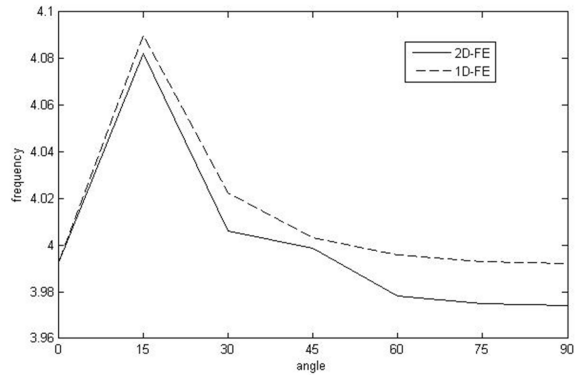


Fig. 12 Effect of Ply angles on First frequency for cantilever beam (a)

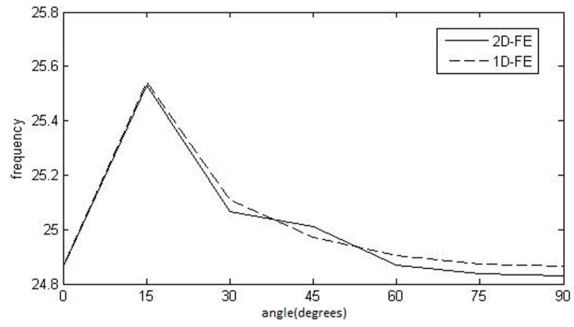


Fig. 13 Effect of Ply angles 2nd frequency for cantilever beam (a)

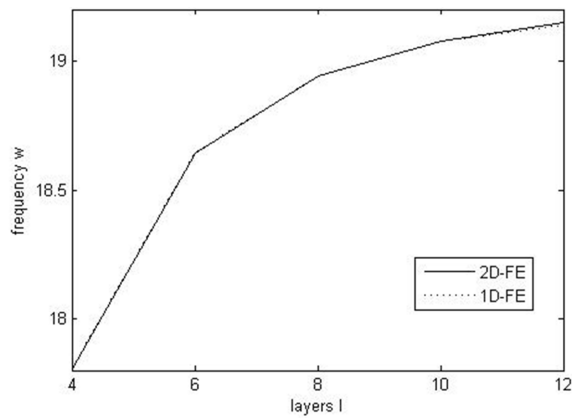


Fig. 14 Effect of number of layers on frequency for cantilever beam (a)

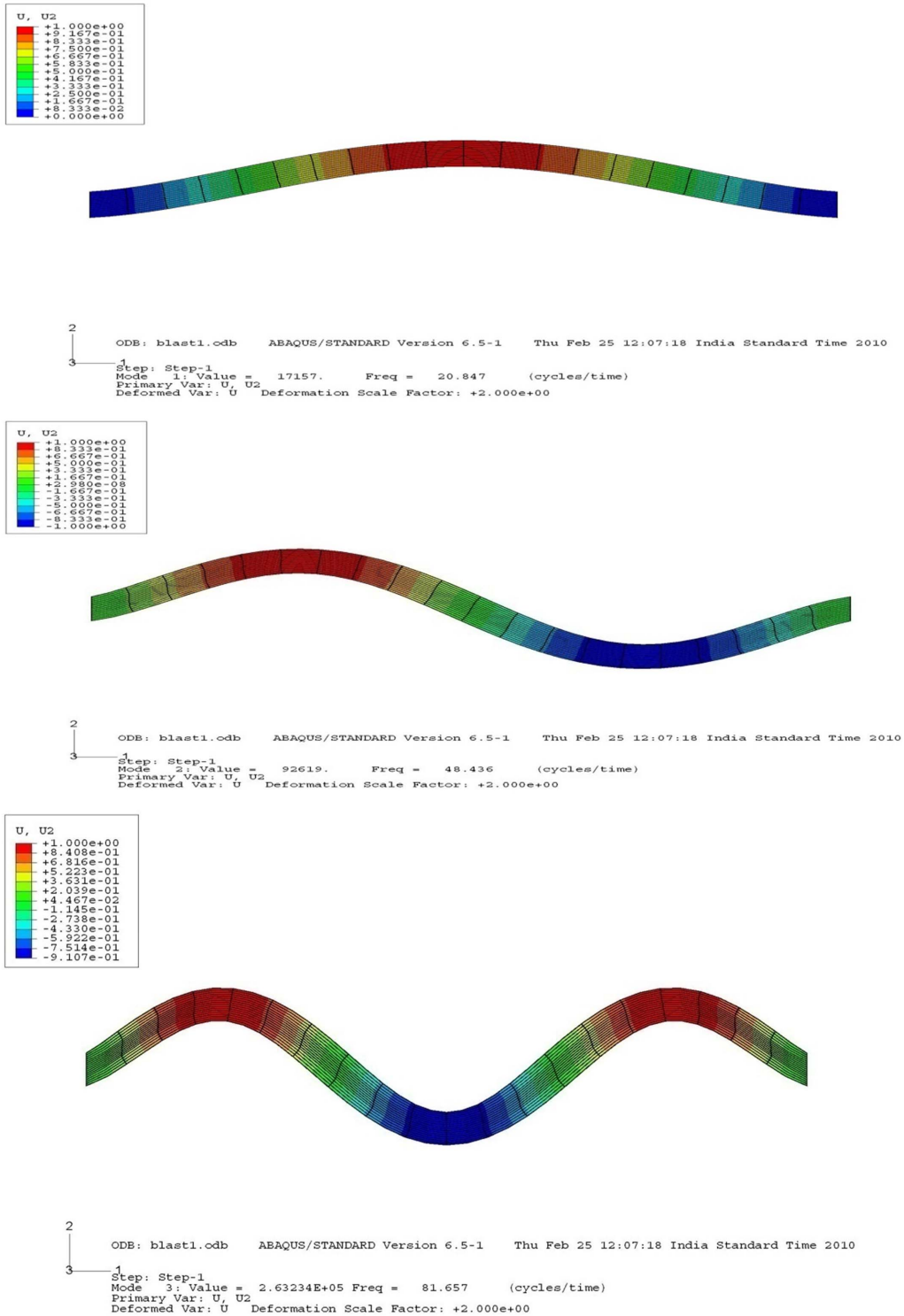


Fig. 15 First three flexural bending modes for fixed Composite beam (b), with $S = 20$

4. Conclusions

The present FE model is developed for dynamic analysis of laminated composite beams for various end conditions for which exact analytical solutions are not present. The presented model is capable of computing dynamic response for various end conditions viz. cantilever and fixed, satisfactorily. The checking of accuracy and validation have been done by comparing the deflection and stress results obtained by this model with that obtained by 2D-FE analysis. The 2D-FE analysis has been done with the help of ABAQUS software package. The comparison shows that the 1D-FE model of zigzag theory yields very accurate results for natural frequencies and mode shapes for cantilever and clamped-clamped (fixed) boundary conditions of laminated composite and sandwich beams with $S \geq 10$. The finite element model is free of shear locking. This work can be extended for obtaining the 1D-FE results for zigzag theory for laminated composite beams for other kind of loading such as static patch load, harmonic patch loads, static sinusoidal load and other end conditions viz. propped, clamped-hinged etc.

Acknowledgements

We are thankful to Professor S. Kapuria, IIT Delhi for his help and guidance.

References

- ABAQUS Documentation (2007), Version 6.6.
- Akhras, G. and Li, W. (2007), "Spline finite strip analysis of composites plates based on higher-order zigzag composites plates", *Compos. Struct.*, **78**, 112-118.
- Arya, H., Shimpi, R.P. and Naik. (2002), "A zigzag model for laminated composite beams", *Compos. Struct.*, **56**, 21-24.
- Averill, R.C. (1994), "Static and dynamic response of moderately thick laminated beams with damage", *Compos. Eng.*, **4**, 381-395.
- Averill, R.C. and Yip, Y.C. (1996), "Thick beam theory and finite element model with zigzag approximation", *AIAA J.*, **34**, 1626-1632.
- Benjeddou, A. (2000), "Advances in piezoelectric finite element modeling of adaptive structural elements: a survey", *Comput. Struct.*, **76**, 347-363.
- Cho, M. and Parmeter, R.R. (1992), "Efficient higher order plate theory for laminated composites", *Compos. Struct.*, **20**(2), 113-123.
- Chopra, I. (2002), "Review of state of art of smart structures and integrated systems", *AIAA J.*, **40**, 2145-2187.
- Fares, M.E. and Elmarghamy, M. Kh. (2008), "A refined zigzag nonlinear first order shear deformation theory of composite laminated plates", *Compos. Struct.*, **82**, 71-83.
- Kapurja S. and Alam, N. (2006), "Efficient layerwise finite element model for dynamic analysis of laminated piezoelectric beams", *Comput. Meth. Appl. Mech. Eng.*, **195**, 2742-2760.
- Kapurja, S. and Achary, G.G.S. (2008), "Benchmark 3D solution and assessment of a zigzag theory for free vibration of hybrid plates under initial electrothermomechanical stress", *Compos. Sci. Technol.*, **68**, 297-311.
- Kapurja, S., Ahmed, A. and Dumir, P.C. (2005), "An efficient coupled zigzag theory for dynamic analysis of piezoelectric composite and sandwich beams with damping", *J. Sound Vib.*, **279**, 345-371.
- Kapurja, S., Bhattacharya, M. and Kumar, A.N. (2008), "Bending and free vibration response of layered functionally graded beams: A theoretical model and its experimental validation", *Compos. Struct.*, **82**, 390-402.
- Kapurja, S., Dumir, P.C. and Jain, N.K. (2004), "Assessment of zigzag theory for static loading, buckling, free

- and forced response of composite and sandwich beams”, *Compos. Struct.*, **64**, 317-327.
- Kumari, P., Nath, J.K., Kapuria, S. and Dumir, P.C. (2008), “An improved third order theory and assessment of efficient zigzag theory for angle-ply flat hybrid panels”, *Compos. Struct.*, **83**, 226-236.
- Mackerle, J. (2003), “Smart materials and structures—a finite element approach—an addendum: a bibliography (1997–2002)”, *Model. Simul. Mater. Sci. Eng.*, **11**, 704-744.
- Noor, A.K. and Burton, W.S. (1994), “Three-dimensional solutions for initially stressed structural sandwiches”, *J. Eng. Mech.-ASCE*, **120**, 284-303.
- Robbins, D.H. and Reddy, J.N. (1991), “Analysis of piezoelectrically actuated beams using a layer-wise displacement theory”, *Comput. Struct.*, **41**, 265-279.
- Tang Y.Y., Noor, A.K. and Xu, K. (1996), “Assessment of computational models for thermoelectroelastic multilayered plates”, *Comput. Struct.*, **61**, 915-933.

Appendix

The elements of the stiffness matrix M^e are computed by exact integration as

$$M^e = \begin{bmatrix} I_{11}c_1 & -I_{12}c_2 & I_{13}c_1 \\ & I_{22}c_3 + \bar{I}_{22}c_4 & -I_{23}c_2^T \\ \text{sym.} & & I_{33}c_1 \end{bmatrix} \quad (31)$$

with

$$\begin{aligned} c_1 &= \int_0^{L_e} N^T \cdot N \cdot dx = \left[\int_0^{L_e} N_i \cdot N_j \cdot dx \right] = \begin{bmatrix} L_e/3 & L_e/6 \\ L_e/6 & L_e/3 \end{bmatrix} \\ c_2 &= \int_0^{L_e} N^T \cdot \bar{N}_{,x} \cdot dx = \left[\int_0^{L_e} N_i \cdot \bar{N}_{j,x} \cdot dx \right] = \begin{bmatrix} -1/2 & L_e/12 & 1/2 & -L_e/12 \\ -1/2 & -L_e/12 & 1/2 & L_e/12 \end{bmatrix} \\ c_3 &= \int_0^{L_e} \bar{N}_{,x}^T \cdot \bar{N}_{,x} \cdot dx = \left[\int_0^{L_e} \bar{N}_{i,x} \cdot \bar{N}_{j,x} \cdot dx \right] \\ &= \begin{bmatrix} 6/5L_e & 1/10 & -6/5L_e & 1/10 \\ 1/10 & 2L_e/15 & -1/10 & -L_e/30 \\ -6/5L_e & -1/10 & 6/5L_e & -1/10 \\ 1/10 & -L_e/30 & -1/10 & 2L_e/15 \end{bmatrix} \\ c_4 &= \int_0^{L_e} \bar{N}^T \cdot \bar{N} \cdot dx = \left[\int_0^{L_e} \bar{N}_i \cdot \bar{N}_j \cdot dx \right] \\ &= \begin{bmatrix} 13L_e/35 & 11L_e^2/210 & 9L_e/70 & -13L_e^2/420 \\ 11L_e^2/210 & L_e^3/105 & 13L_e^2/420 & -L_e^3/140 \\ 9L_e/70 & 13L_e^2/420 & 13L_e/35 & -11L_e^2/210 \\ -13L_e^2/420 & -L_e^3/140 & -11L_e^2/210 & L_e^3/105 \end{bmatrix} \end{aligned} \quad (32)$$

The elements of the stiffness matrix K^e are computed by exact integration as

$$K^e = \begin{bmatrix} A_{11}c_5 & -A_{12}c_6 & A_{13}c_5 \\ & A_{22}c_7 & A_{33}c_6^T \\ \text{sym.} & & A_{33}c_5 + \bar{A}_{33}c_1 \end{bmatrix} \quad (33)$$

with

$$\begin{aligned} c_5 &= \int_0^{L_e} N_{,x}^T \cdot N_{,x} \cdot dx = \left[\int_0^{L_e} N_{i,x} \cdot N_{j,x} \cdot dx \right] = \begin{bmatrix} 1/L_e & -1/L_e \\ -1/L_e & 1/L_e \end{bmatrix} \\ c_6 &= \int_0^{L_e} N_{,x}^T \cdot \bar{N}_{,xx} \cdot dx = \left[\int_0^{L_e} N_{i,x} \cdot \bar{N}_{j,xx} \cdot dx \right] = \begin{bmatrix} 0 & 1/L_e & 0 & -1/L_e \\ 0 & -1/L_e & 0 & 1/L_e \end{bmatrix} \end{aligned}$$

$$\begin{aligned}
c_7 &= \int_0^{L_e} \bar{N}_{,xx}^T \cdot \bar{N}_{,xx} \cdot dx = \left[\int_0^{L_e} \bar{N}_{i,xx} \cdot \bar{N}_{j,xx} \cdot dx \right] \\
&= \begin{bmatrix} 12/L_e^3 & 6/L_e^2 & -12/L_e^3 & 6/L_e^2 \\ 6/L_e^2 & 4/L_e & -6/L_e^2 & 2/L_e \\ -12/L_e^3 & -6/L_e^2 & 12/L_e^3 & -6/L_e^2 \\ 6/L_e^2 & 2/L_e & -6/L_e^2 & 4/L_e \end{bmatrix} \quad (34)
\end{aligned}$$

p_z^1, p_z^2 are linearly interpolated in terms of their nodal values, i.e.

$$p_z^1 = N \cdot p_z^{1e}, \quad p_z^2 = N \cdot p_z^{2e} \quad (35)$$

with

$$p_z^{1e} = \begin{bmatrix} p_{z_1}^1 \\ p_{z_2}^1 \end{bmatrix}, \quad p_z^{2e} = \begin{bmatrix} p_{z_1}^2 \\ p_{z_2}^2 \end{bmatrix} \quad (36)$$

Substituting $B_{m_2}^T$ from Eq. (20) into Eq. (26) yields

$$P^e = \int_0^{L_e} B_{m_2}^T \cdot F_2 \cdot dx = \int_0^{L_e} \begin{bmatrix} 0 \\ \bar{N}^T \cdot F_2 \\ 0 \end{bmatrix} \cdot dx \quad (37)$$

where

$$F_2 = b \cdot N \cdot p_z^e, \quad p_z^e = \begin{bmatrix} p_{z_1} \\ p_{z_2} \end{bmatrix} = p_z^{1e} + p_z^{2e} \quad (38)$$

Substituting F_2 from Eq. (38) into Eq. (37) yields the element load vector P^e as

$$P^e = \begin{bmatrix} 0 \\ c_8 \cdot p_z^e \\ 0 \end{bmatrix} \quad (39)$$

Where

$$c_8 = b \int_0^{L_e} \bar{N}^T \cdot N \cdot dx = \begin{bmatrix} \int_0^{L_e} b \cdot \bar{N}_i \cdot N_j \cdot dx \end{bmatrix} = \begin{bmatrix} 7bL_e/20 & 3bL_e/20 \\ bL_e^2/20 & bL_e^2/30 \\ 3bL_e/20 & 7bL_e/20 \\ -bL_e^2/30 & -bL_e^2/20 \end{bmatrix} \quad (40)$$

Notations

L, L_e	: Number of layers, Length of Finite Element
σ, ε	: Stress, Engineering Strain
$\sigma, \tau_{ij}, \varepsilon_i, \gamma_{ij}$: Normal & Shear Stresses and Strain Components
$Y_i, G_{ij}, \nu_{ij}, \rho$: Elastic & Shear Moduli, Poission's Ratio, density
a, b, h, S	: Length, Width & Thickness of Beam, Span to thickness Ratio
u, w, ψ	: Axial & Transverse Displacement and Shear Rotation
x, y, z	: Axial, Width and thickness Coordinates
z_{k-1}	: coordinate of the Lower Face of k th Layer
Q_{ii}	: Transformed reduced Stiffnesses
$R^k(z), R^{kl}(z)$: Function of u in k th Layer
p_z^1, p_z^2, F_2	: Transverse Loads
$I_{ij}, \bar{I}_{ij}, I_{ib}, \bar{I}_{il}$: Inertia Element
N_x, M_x, P_x, Q_x, V_x	: Stress Resultants
A_{ij}, \bar{A}_{ij}	: Beam Stiffness Element
\bar{U}, \bar{P}	: Displacement and Load Vector
$\bar{w}, \bar{\omega}_n$: Dimensionless Deflection & Natural Frequency
N, \bar{N}	: Interpolation Function
$\hat{I}, \hat{F}, \hat{D}, \hat{B}$: Generalized Inertia, Stress, Stiffness & Strain Matrix
M^e, K^e, P^e	: Elemental Mass, Stiffness & Load Matrix